A Linearized Theory for Swirling Supersonic Jets and Its Application to Shock-Cell Noise

P.W. Carpenter*
University of Exeter, Exeter, England

A linearized theory is developed for underexpanded inviscid supersonic jets with arbitrary initial swirl. The radial displacement of a given streamline from its position at the nozzle exit is used as the dependent variable. The governing equation is fairly complicated and has to be solved numerically by the method of characteristics. A simple expression for the wavelength of the primary shock cell is derived. The linearized theory is used to extend some of Howe and Ffowcs Williams' theoretical results for shock-associated noise to swirling supersonic jets. In this way, estimates are made of the effect of swirl on the total radiated sound power of shock-associated noise. It is found that for a certain type of swirl the shock-associated noise can be greatly reduced, or even eliminated, for sufficiently high swirl levels. This can be achieved at the expense of a very small thrust loss.

Nomenclature

a = local speed of sound
a_* = critical speed of sound
A = see Eq. (42)
b = width of mixing layer
B = stagnation enthalpy
f_p = peak frequency
F_i = see Eqs. (15) and (16) for $i = 1$ and 2, respectively
M_a = w_c/a_a
M_J = q_J/a_{bJ}
M_w = w_b/a_b
p = static pressure
p_0 = stagnation pressure
$\overline{p^2}$ = mean square pressure fluctuation in far field
P = energy flux from coherent field into random field in mixing layer
P_1 = component of P, see Eq. (41)
P_2 = component of P, see Eq. (44)
P_a = total energy flux of radiated sound in moving reference frame
P_T = total sound power
$\boldsymbol{q}$ = velocity vector
Q = q_b/a_*
r = radial coordinate of a given streamline
r_1 = radial coordinate of a given streamline at nozzle exit
R = radius of a large sphere centered at nozzle exit
R_i, R_o = radial coordinate of inner and outer edge of mixing layer, respectively
R_N = nozzle exit radius
t = time
u, v, w = radial, swirl, and axial velocity components, respectively
U = u/a_*
V = v/a_*
w_c = axial component of eddy convection velocity
W = w/a_*
z = axial coordinate
z_1 = $z - w_c t$
γ = ratio of specific heats
δU = $U - U_b$
δV = $V - V_b$
δW = $W - W_b$
Δ = $r - r_1$
Δp_e = pressure difference between nozzle lip and ambient
ϵ = $W_{bJ} - W_{ex}$
ϵ_T = $\sqrt{\langle \xi^2 \rangle}/a_{bJ}$
ζ_c = nondimensional core radius of inner-biased swirling (IBS) flow
ζ_c^* = nondimensional core radius of outer-biased swirling (OBS) flow
θ = angle of observation, see Fig. 4
θ_p = peak noise angle
λ = wavelength of primary shock cell
ξ = circulation density along mixing layer
ρ = density
ρ_0 = stagnation density
ϕ = azimuthal coordinate
ω = vorticity in mixing layer
$\overline{(\ )}$ = coherent field variable
$(\ )'$ = random field variable
$\langle\ \rangle$ = ensemble average of turbulent fluctuations

Subscripts

a = ambient conditions
b = basic unperturbed flow
e = conditions at nozzle lip
J = conditions on jet boundary
x = nozzle exit conditions
0 = no swirl

Presented as Paper 80-1449 at the AIAA 13th Fluid and Plasma Dynamics Conference, Snowmass, CO, July 14-16, 1980; received Oct. 29, 1984; revision received May 2, 1985.

*Lecturer, Engineering Science Department. Member AIAA.

I. Introduction

When a supersonic nozzle flow is underexpanded, i.e., the exit pressure exceeds the ambient pressure, a characteristic pattern of shock cells is formed. This is depicted in Fig. 1. Several noise generation mechanisms involving these shock cells have been postulated and, in some cases, investigated experimentally. These include screech, noise arising from instabilities of the turbulent jet, and shock-associated noise.

Screech, as shown by Powell,[1] is essentially caused by acoustic feedback. The turbulent eddies interact with the shock waves at the end of the shock cells, generating sound waves that propagate upstream in the ambient medium and trigger the release of a new eddy at the nozzle exit. This produces an intense sound consisting of discrete tones only. Screech is not usually observed in hot jets. Tam[2] postulated a mechanism for broadband noise whereby waves generated by the shock-cell structure propagate downstream and give rise to instabilities in the main part of the turbulent jet downstream of the potential core.

Shock-associated noise is also generated by the interaction of the turbulent eddies with the quasiperiodic shock-cell structure. Unlike screech, however, it has a broadband but strongly peaked sound field. Harper Bourne and Fisher[3] have investigated this noise experimentally. They have also developed a successful semiempirical theory for the phenomenon. More recently, Howe and Ffowcs Williams[4] have presented an ingenious analytical theory for shock-associated noise. The main purpose of the present paper is to show how some of their results may be extended to supersonic swirling jets.

Howe and Ffowcs Williams model the shock-cell structure by adapting certain results obtained from the linearized theory for supersonic jets. So, in order to extend their theory to swirling jets, it is necessary first to develop a linearized theory for inviscid swirling jets. Section II of this paper is devoted to a presentation of such a theory. In Sec. III, this theory is used to predict the effect of swirl on the total sound power of shock-associated noise. The theoretical results and their implications are discussed in Sec. IV. The main conclusions and results are summarized in Sec. V. It is found that, for a certain type of swirl, shock-associated noise may be greatly reduced, or even eliminated, at the cost of no more than a 1-2% thrust loss.

II. Linearized Theory for Supersonic Swirling Jets

Choice of Perturbation Variables

The well-known linearized theory due to Prandtl[5] and Pack[6] uses a velocity potential as the perturbation variable. Since swirling flows are, in general, rotational, a velocity potential can no longer be used. In principle, a stream function ψ could be used. However, in practice, the swirl distribution would be given at the nozzle exit and there would be practical difficulties in expressing this initial swirl profile as a function of ψ. For this reason, the quasi-Lagrangian coordinates introduced by Carpenter and Johannesen[7] are used. To be specific, the radial displacement Δ of a given streamline from its initial radial position r_1 is used as the dependent variable, with r_1 and the axial distance z downstream from the nozzle exit as the independent variables. Thus, z is analogous to time in a one-dimensional Lagrangian coordinate system. The coordinate system adopted for the linearized theory is illustrated in Fig. 2.

Nozzle Exit Conditions and Basic Unperturbed Flow

Let us assume that the swirl is produced by means of stationary vanes. This implies that, to a good approximation, the entropy and stagnation enthalpy will be constant throughout the jet flow. Consequently, the Crocco vorticity equation reduces to

$$\boldsymbol{q} \times \operatorname{curl} \boldsymbol{q} = 0 \tag{1}$$

where $\boldsymbol{q}$ is the velocity vector.

For an axisymmetric swirling flow the three components of Eq. (1) are given by

$$w\left(\frac{\partial u}{\partial z} - \frac{\partial w}{\partial r}\right) = \frac{v}{r}\frac{\partial (rv)}{\partial r} \tag{2}$$

$$u\left(\frac{\partial u}{\partial z} - \frac{\partial w}{\partial r}\right) = \frac{v}{r}\frac{\partial (rv)}{\partial z} \tag{3}$$

$$rv = \text{const along a streamline} \tag{4}$$

where (u, v, w) are the components of $\boldsymbol{q}$ in the (r, ϕ, z) directions.

At this point, it is convenient to introduce the nondimensional velocity components

$$U = u/a_*, \quad V = v/a_*, \quad W = w/a_* \tag{5}$$

where a_* is the critical speed of sound.

Let us assume that the flow at the nozzle exit is equivalent to an inviscid swirling flow in an infinitely long pipe of circular cross section. In this case, integration of Eq. (2) gives

$$W_x = \left[W_{ex}^2 + 2\int_{r_1}^{R_N} \frac{V_x}{r_1'} \frac{\mathrm{d}(V_x r_1')}{\mathrm{d}r_1'} \mathrm{d}r_1' \right]^{\frac{1}{2}} \tag{6}$$

where suffix x denotes conditions at nozzle exit and $W_{ex} \equiv W_x(R_N)$. Thus, if W_{ex} and V_x are given, the axial velocity profile at nozzle exit can be determined from Eq. (6).

For supercritical flow in a convergent-divergent nozzle, the value of W_{ex} depends on the ratio of the nozzle exit and

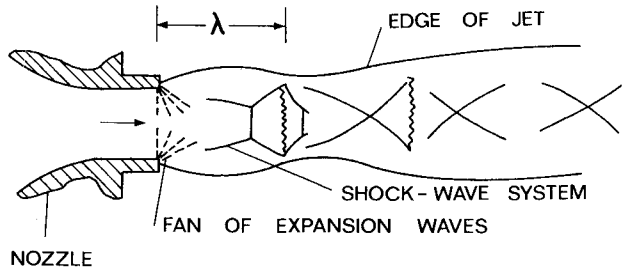

Fig. 1 Shock-cell structure.

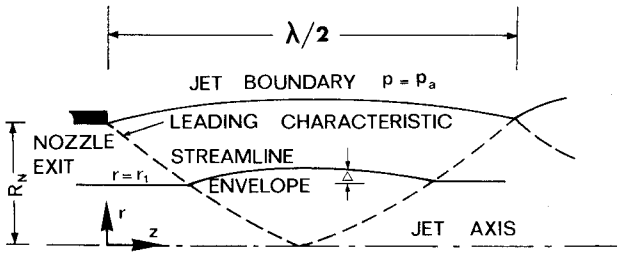

Fig. 2 Coordinate system for supersonic jet.

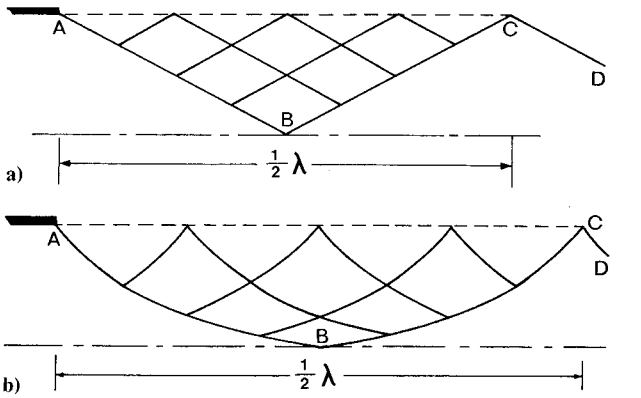

Fig. 3 Characteristics in the (r_1, z) plane: a) nonswirling axisymmetric flow; b) swirling flow.

throat areas. The actual determination of W_{ex} is fairly involved and is explained in Refs. 7 and 8.

For a convergent nozzle, it is somewhat simpler. In this case, as explained in Refs. 7, 9, and 10, W_{ex} is set equal to the local speed of sound. By means of the isentropic flow relations, we can then derive the following simple result:

$$W_{ex} = \left(1 - \frac{\gamma - 1}{\gamma + 1} V_{ex}^2\right)^{\frac{1}{2}} \tag{7}$$

where γ is the ratio of the specific heats. Equation (7) is equivalent to Eq. (29) of Ref. 9.

We now need to choose the basic unperturbed flow. For a nonswirling jet, Pack[6] chose a basic flow with a uniform axial velocity equal to the constant velocity on the jet boundary. It is desirable to extend this approach to the swirling jet. So, denoting the properties of the basic flow by use of the suffix b, the undisturbed swirl velocity V_b is chosen as

$$V_b = V_x \tag{8}$$

and, in a similar fashion to Eq. (6), the axial velocity is given by

$$W_b = \left[Q_J^2 - V_{bJ}^2 + 2\int_{r_1}^{R_N} \frac{V_b}{r_1'} \frac{\mathrm{d}(V_b r_1')}{\mathrm{d}r_1'}\, dr_1'\right]^{\frac{1}{2}} \tag{9}$$

where $Q = |q|/a_*$ and suffix J denotes conditions on the jet boundary, i.e., at $r_1 = R_N$. Equations (8) and (9) imply that

$$V_{bJ}^2 + W_{bJ}^2 = Q_J^2 \tag{10}$$

which shows that Eqs. (8) and (9) represent the appropriate extension of Pack's basic flow.

Velocity Perturbations in Terms of Δ

If higher-order terms are systematically neglected, the radial and swirl velocity perturbations are readily obtained. From the definition of a streamline we obtain

$$U = W_b \partial\Delta/\partial z \tag{11}$$

Use of Eq. (4) leads to

$$\delta V \equiv V - V_b = -V_b \Delta / r_1 \tag{12}$$

The application of continuity to a stream tube gives

$$\rho W r\, \mathrm{d}r = \rho_x W_x r_1\, \mathrm{d}r_1 \tag{13}$$

where ρ is the density.

By use of Eq. (12) and systematic neglect of higher-order terms, Eq. (13) can be rearranged to give

$$\delta W \equiv W - W_b = -\frac{F_1}{r_1}\Delta - F_2 \frac{\partial \Delta}{\partial r_1} - \epsilon \tag{14}$$

where

$$F_1 = \frac{\rho_b W_b - W_b V_b (\partial \rho_b / \partial V_b)}{\rho_b + W_b (\partial \rho_b / \partial W_b)} \tag{15}$$

$$F_2 = \frac{\rho_b W_b}{\rho_b + W_b (\partial \rho_b / \partial W_b)} \tag{16}$$

and

$$\epsilon = W_{bJ} - W_{ex} \tag{17}$$

By using the isentropic flow relations, it can be shown that

$$\frac{\partial \rho_b}{\partial V_b} = -\frac{2 V_b \rho_b}{(\gamma + 1)\Lambda}, \quad \frac{\partial \rho_b}{\partial W_b} = -\frac{2 W_b \rho_b}{(\gamma + 1)\Lambda} \tag{18}$$

where

$$\Lambda = 1 - \frac{\gamma - 1}{\gamma + 1}\left(W_b^2 + V_b^2\right) \tag{19}$$

Derivation of Governing Equation

The nondimensional axial velocity difference ϵ at the nozzle lip may be regarded as the fundamental small parameter. In essence, the governing equation is derived from Eq. (2) by changing variables from (r, z) to (r_1, z) and neglecting terms of $\mathcal{O}(\epsilon^2)$. Carrying out this procedure transforms Eq. (2) to

$$W_b \frac{\partial U}{\partial z} = \left[W \frac{\partial W}{\partial r_1} + \frac{V_b r_1}{r^2} \frac{\mathrm{d}(r_1 V_b)}{\mathrm{d}r_1}\right]\left(\frac{\partial r_1}{\partial r}\right)_z \tag{20}$$

Now

$$\left(\frac{\partial r_1}{\partial r}\right)_z = 1 + \mathcal{O}(\epsilon) \tag{21}$$

It follows also from Eq. (9) that

$$W_b \frac{\mathrm{d}W_b}{\mathrm{d}r_1} = -\frac{V_b r_1}{r_1^2} \frac{\mathrm{d}(V_b r_1)}{\mathrm{d}r_1} \tag{22}$$

Recalling that $r = r_1 + \Delta$, using Eqs. (11), (21), and (22), and neglecting terms of $\mathcal{O}(\epsilon^2)$, Eq. (20) becomes

$$W_b^2 \frac{\partial^2 \Delta}{\partial z^2} = W \frac{\partial W}{\partial r_1} - W_b \frac{\partial W_b}{\partial r_1} - \frac{2 V_b r_1}{r_1^3} \frac{\mathrm{d}(V_b r_1)}{\mathrm{d}r_1} \Delta \tag{23}$$

Finally, after setting $W = W_b + \delta W$, substituting for δW from Eq. (14), neglecting terms of $\mathcal{O}(\epsilon^2)$, and a certain amount of algebraic manipulation and rearrangement, Eq. (23) becomes

$$\frac{\partial^2 \Delta}{\partial z^2} - \frac{1}{M_w^2 - 1}\left(\frac{\partial^2 \Delta}{\partial r_1^2} + \frac{F_3}{r_1}\frac{\partial \Delta}{\partial r_1} - \frac{F_4}{r_1^2}\Delta\right) - F_5 = 0 \tag{24}$$

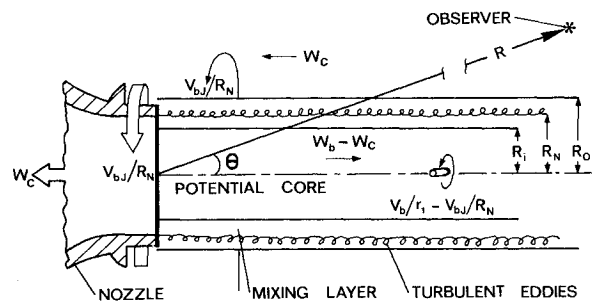

Fig. 4 Model problem for shock-cell noise.

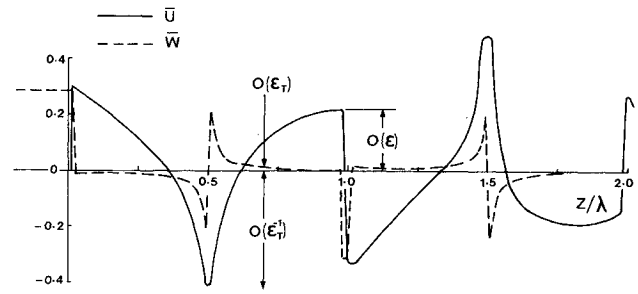

Fig. 5 Distributions of $\bar{w}$ and $\bar{u}$ along $r_1 = R_i$ for small ϵ_T.

where

$$M_w(r_1) = W_b/a_b$$

$$F_3(r_1) = -\left(M_w^2 - 1\right)\left[\frac{F_1}{W_b} + \frac{r_1}{W_b^2}\cdot\frac{\mathrm{d}(W_b F_2)}{\mathrm{d}r_1}\right]$$

$$F_4(r_1) = -\left(M_w^2 - 1\right) \times\left[\frac{r_1^2}{W_b}\frac{\mathrm{d}}{\mathrm{d}r_1}\left(\frac{F_1}{r_1}\right) + \frac{r_1 F_1}{W_b^2}\frac{\mathrm{d}W_b}{\mathrm{d}r_1} + \frac{2V_b}{W_b^2}\frac{\mathrm{d}(r_1 V_b)}{\mathrm{d}r_1}\right]$$

$$F_5(r_1) = \frac{\epsilon}{2W_b^3}\cdot\frac{\mathrm{d}(V_b r_1)^2}{\mathrm{d}r_1}$$

Boundary Condition on Jet Boundary

The pressure must remain constant on the jet boundary where $r_1 = R_N$. This implies that

$$W^2 + V^2 = W_b^2 + V_b^2 \text{ at } r_1 = R_N \tag{25}$$

Using Eqs. (12) and (14) and neglecting terms of $\mathcal{O}(\epsilon^2)$, Eq. (25) becomes

$$\left(V_{bJ}^2 + W_{bJ}F_1\right)\Delta_J + W_{bJ}F_2\left(\frac{\partial\Delta_J}{\partial r_1}\right) + \epsilon W_b = 0 \tag{26}$$

Solution of Governing Equation

The governing equation (24) is fairly complicated and there seems little prospect of an analytical solution. However, no special difficulties are involved in integrating the equation numerically by means of the method of characteristics. Since the equation is linear, the characteristics are known a priori and are given by

$$\mathrm{d}z/\mathrm{d}r_1 = \pm\left(M_w^2 - 1\right)^{\frac{1}{2}} \tag{27}$$

For swirling flow, M_w varies across the jet so the characteristics are curved. This is illustrated in Fig. 3 where the swirling and nonswirling cases are compared.

One important result can be obtained immediately by inspection of Fig. 3. It follows from geometrical considerations that the wavelength of a shock cell in a swirling jet is given by

$$\lambda = 4R_N\int_0^1\left(M_W^2 - 1\right)^{\frac{1}{2}}\mathrm{d}r_1 \tag{28}$$

There may be some doubt as to whether the factor 4 is the correct choice in Eq. (28). This point can be resolved by noting that the characteristic AB in Fig. 3a represents an expansion fan that should reflect from the axis of symmetry as another expansion BC. BC should then reflect from the jet boundary as a compression wave. This suggests that the basic wavelength of the pressure field is indeed given by Eq. (28). Actually, matters are not quite that straightforward. The perturbation velocity U tends to infinity as B is approached along AB. Moreover, characteristics BC and CD are lines of logarithmic singularities in U. Nevertheless, Fig. 1 of Grabitz[11] clearly shows that the wavelength of the pressure field is given by Eq. (28) in a nonswirling jet. The discrepancy with Pack's[6] formula for λ is also similarly explained. Pack defined the end of the primary shock cell as coinciding with the first minimum in the jet boundary. It turns out that this minimum does not correspond to any significant feature of the pressure field. These matters are discussed more fully in Ref. 12 for the nonswirling case. When swirl is present, the essential features remain unchanged, but with curved (rather than straight) characteristics.

III. Theory for Shock-Associated Noise

The object of the theory presented in this section is limited to the prediction of the effects of swirl on the peak frequency and total radiated sound power of shock-associated noise. It is achieved by adapting some of Howe and Ffowcs Williams' results to deal with a supersonic swirling jet.

For present purposes, the theory as set out in Ref. 4 can be considered to consist of three main steps:

1) A model problem is defined in a moving reference frame in which the shock-cell pattern moves upstream and interacts with frozen turbulent eddies instead of the real situation where the eddies are convected downstream and interact with a stationary shock-cell pattern.

2) Equations for the acoustic variables are derived and solved for the model problem.

3) The results for such quantities as mean square pressure fluctuation in the far field and sound power have to be transformed back to the real coordinate system. In Ref. 4, these steps are by no means similar in magnitude, i.e., step 2 requires a great deal of detailed analysis. Fortunately, it turns out that the limited goals of the present paper can be realized without significant modification of much of this analysis.

Definition of Model Problem

The idealization assumed for the turbulent mixing layer in a swirling jet is described below. The mixing layer is assumed to be at constant density ρ_{bJ} and to be confined to a thin region of constant thickness b having an inner radius of R_i and an outer radius of R_o. (See Fig. 4.) The turbulent eddies are modeled by a continuum of vortex rings of radius R_N, which are simultaneously rotating at an angular velocity v_{bJ}/R_N and being convected downstream at velocity w_c. According to the experimental data of Harper Bourne and Fisher,[3] $w_c \simeq 0\cdot 7\, w_{bJ}$ for a cold nonswirling supersonic jet. In the absence of any other information, this value is assumed to hold for both cold and hot swirling supersonic jets.

The analysis is carried out in a reference frame in which the turbulent eddies are stationary, i.e., the turbulence is frozen. Thus, a new coordinate system (r_1, ϕ_1, z_1) is defined such that

$$\phi_1 = \phi - v_{bJ}t/R_N, \quad z_1 = z - w_c t \tag{29}$$

The shock-cell pattern along with the ambient medium is now conceived to be moving to the left at velocity w_c and simultaneously rotating with angular speed v_{bJ}/R_N. The flow in the potential core is moving to the right at velocity $(w_b - w_c)$ and rotating at variable angular speed $(v_b/r_1 - v_{bJ}/R_N)$.

In this new coordinate system, the stationary turbulent eddies are represented by a vorticity distribution of the form,

$$\omega = \xi(z_1)\,\delta(r_1 - R_N)\,\hat{e}_\phi \tag{30}$$

where $\delta(x)$ is the Dirac delta function and $\hat{e}_\phi$ a unit vector in the azimuthal direction. The circulation density ξ is assumed to be a stationary random function of z_1 with zero mean.

In terms of the moving coordinate system, the jet boundary now becomes a perturbation pressure wave of the form

$$\bar{p} = -\Delta p_e H(z_1 + w_c t) \tag{31}$$

where Δp_e is the difference between the pressure at the nozzle lip and ambient and $H(x)$ the Heaviside step function.

The interaction of the turbulent eddies and the shock-cell structure results in the gradual decay of the latter with distance downstream of the nozzle exit. With the original coordinate system, it is not really feasible to attempt to calculate the corresponding rate of energy transfer to the random sound field. However, in the moving reference frame, it is fairly easy to make an estimate of the total rate of energy transfer to the random field in the mixing layer. Since the turbulence is independent of time in this reference frame, it follows that all

this energy is converted into sound and trapped internal waves.

Energy Flux into Random Disturbances

Following Ref. 4, the stagnation enthalpy

$$B = p/\rho + \tfrac{1}{2}|\boldsymbol{q}|^2 \tag{32}$$

is adopted as the fundamental acoustic perturbation variable.

For present purposes, the approximate solution to the model problem may be considered as involving two small parameters: one is a measure of the nondimensional pressure difference, say the ϵ introduced in Eq. (17); the other represents a turbulent Mach number, say

$$\epsilon_T = \sqrt{\langle \xi^2 \rangle}/a_{bJ} \tag{33}$$

where the angle brackets denote an average over an ensemble of realizations of the turbulent fluctuations. Note that the limit $\epsilon_T \to 0$ implies that the mixing layer width $b \to 0$.

The perturbation field variables are formally partitioned into a coherent and a random part, e.g.,

$$p(r_1, z_1, t) - p_b(r_1) = \bar{p}(r_1, z_1, t) + p'(r_1, z_1, t) \tag{34}$$

Analogous expressions for the velocity components and stagnation enthalpy are also introduced. (Note that the perturbations are relative to the basic undisturbed state, as defined in Sec. II, transformed to the moving coordinate system.) The overbar in Eq. (34) denotes the coherent or mean component of the field defined as the average with respect to an ensemble of realizations of the turbulent fluctuation ξ. For ϵ and $\epsilon_T \to 0$, the coherent field is given by the linearized theory outlined in Sec. II. Primed quantities, such as p' in Eq. (34), represent the random fluctuations about the mean state resulting from the interaction of the coherent shock-cell structure and the turbulent eddies.

An integral energy equation for the random field within the mixing layer takes the form [see Eq. (7.15) of Ref. 4] of

$$\frac{\partial}{\partial t}\int \frac{1}{2}\left(\rho_{bJ}\langle q'^2 \rangle + \frac{\langle p'^2 \rangle}{\rho_{bJ} a_{bJ}^2} \right) \mathrm{d}\sigma + \oint \rho_{bJ}\langle B'\boldsymbol{q}' \rangle \cdot \boldsymbol{n}\, \mathrm{d}S = P \tag{35}$$

where $\mathrm{d}\sigma$ is a volume element, $\mathrm{d}S$ an areal element on the surface of the mixing layer, $\boldsymbol{n}$ the unit normal directed outward from the mixing layer, q' the magnitude of $\boldsymbol{q}'$, and

$$P = -\int \rho_{bJ}\langle \boldsymbol{q}' \cdot \boldsymbol{\omega} \wedge \bar{\boldsymbol{q}} \rangle \, \mathrm{d}\sigma \tag{36}$$

The first term on the left-hand side of Eq. (35) represents the rate of change of the mean energy associated with the random field within the mixing layer. The surface integral represents the net flux of random energy passing from the mixing layer as sound radiated into the ambient medium or internal waves trapped in the potential core of the jet. The term P on the right-hand side of Eq. (35) represents the source of energy for the random field in the mixing layer. It stems from the interaction between the coherent field $\bar{\boldsymbol{q}}$, the turbulent fluctuations $\boldsymbol{\omega}$, and the random field $\boldsymbol{q}'$, which brings about an energy transfer from the coherent field to the random scattered disturbances.

Howe and Ffowcs Williams showed that P can be rewritten in the form

$$P = -2\pi R_N \rho_{bJ} \int_{-\infty}^{\infty} (\bar{u}\bar{B})_{r=R_i}\, \mathrm{d}z_1 \tag{37}$$

which can now be seen to represent explicitly the energy flux from the coherent field into the mixing layer.

Now for $b \to 0$,

$$\begin{aligned} \bar{B} &= B - B_b = B - p_b/\rho_b - \tfrac{1}{2}(w_b - w_c)^2 \\ &= \bar{p}/\rho_b + (w_b - w_c)\bar{w} \end{aligned} \tag{38}$$

But for $\epsilon \to 0$, $\bar{p}$ and $\bar{w}$ are given by linearized theory, so

$$\bar{p} = -\rho_b(w_b\bar{w} + v_b\bar{v}) \tag{39}$$

In the limit $\epsilon \to 0$, $\bar{w}$ and $\bar{v}$ are identical to $a_* \, \delta W$ and $a_* \, \delta V$, respectively. Thus, using Eq. (12) to substitute for $\bar{v}$ in Eq. (39) and then substituting Eq. (39) for $\bar{p}$ in Eq. (38), allows Eq. (37) to be written as

$$\begin{aligned} P = -2\pi R_N \rho_{bJ} \Bigg[& \frac{w_c}{\rho_{bJ} w_{bJ}} \int_{-\infty}^{\infty} (\bar{u}\bar{p})_{r_1=R_i}\, \mathrm{d}z_1 \\ & + \left(1 - \frac{w_c}{w_{bJ}}\right) v_{bJ}^2 \int_{-\infty}^{\infty} \left(\frac{\bar{u}\Delta}{r_1}\right)_{r_1=R_i} \mathrm{d}z_1 \Bigg] \end{aligned} \tag{40}$$

The evaluation of the two integrals on the right-hand side of Eq. (40) will now be considered.

In the limit as $\epsilon_T \to 0$, $R_i \to R_N$ and $\bar{p}$ takes the form of the step function in Eq. (31). So the only difference between the swirling and nonswirling cases would be the value of Δp_e. On the other hand, provided ϵ is small, typical distributions of normal velocity $\bar{u}$ along the jet boundary take the form shown in Fig. 5. Most of the difference between the $\bar{u}$ distributions for the swirling and nonswirling cases can be accounted for by the reduction in Δp_e that occurs with swirl. However, some differences in shape may be discerned. The dominant feature in all cases is the existence of a logarithmic singularity[11] at $z = \frac{1}{2}\lambda$ (additional singularities occur at $z = 3/2\lambda, 5/2\lambda, \ldots$). For small but finite ϵ_T, the distributions $\bar{w}$ (i.e., $-\bar{p}/\rho_b w_b$) and $\bar{u}$ along $r_1 = R_i$ are shown schematically in Fig. 5. It is clear from Fig. 5 that the value of the integral in the first term on the left-hand side of Eq. (40), viz.,

$$P_1 = -2\pi R_N \left(\frac{w_c}{w_{bJ}}\right) \int_{-\infty}^{\infty} (\bar{u}\bar{p})_{r_1=R_i}\, \mathrm{d}z_1 \tag{41}$$

is heavily dependent on the behavior of $\bar{u}$ in the neighborhood of the singularities at $z = \lambda/2$, etc. Let us assume that near $z = \lambda/2$,

$$\bar{u} \sim \epsilon A \ell n |\lambda/2 - z| \tag{42}$$

A and λ will vary with the degree and type of swirl. It is now argued that to a good approximation

$$\frac{P_1}{(P)_0} = \frac{\lambda A \, \Delta p_e \, \Delta w_e}{(\lambda A \, \Delta p_e \, \Delta w_e)_0} \tag{43}$$

where $(\ \ )_0$ denotes nonswirling flow.

Since the second term of Eq. (40), viz.,

$$P_2 = -2\pi R_N \rho_{bJ} v_{bJ}^2 \left(1 - \frac{w_c}{w_{bJ}}\right) \int_{-\infty}^{\infty} \left(\frac{\bar{u}\Delta}{r_1}\right)_{r_1=R_i} \mathrm{d}z_1 \tag{44}$$

is $\mathcal{O}(v_{bJ}^2)$, it is likely to be small compared to P_1. Therefore, to an acceptable approximation, Howe and Ffowcs Williams' expressions for $\bar{u}$ and Δ may be used [i.e., Eqs. (26) and (10), respectively, of Ref. 4]. Then a fairly similar procedure to that used in Ref. 4 to evaluate the integral in P_1 may be used to obtain

$$\int_{-\infty}^{\infty} \left(\frac{\bar{u}\Delta}{r_1}\right)_{r_1=R_N} \mathrm{d}z_1 = \frac{\lambda^4 (\Delta p_e)^2}{256\pi R_N^3 \rho_{bJ}^2 w_{bJ}^3} \sum_{n=1}^{\infty} \frac{1}{j_{0n}^4} \tag{45}$$

where j_{0n} is the nth positive zero of the Bessel function $J_0(x)$. The infinite sum in Eq. (45) is approximately equal to 0.0312. Using the expression for $(P_1)_0$ given as Eq. (2.31) of Ref. 4 leads to the following estimate:

$$\frac{P_2}{(P)_0} = -\frac{0.0312\lambda^2}{4\pi}\left(\frac{v_{bJ}}{w_{bJ}}\right)^2\left(\frac{w_{bJ}}{w_c}-1\right)\frac{(w_{bJ})_0(\Delta p_e)^2}{w_{bJ}\left[(\Delta p_e)^2\right]_0} \tag{46}$$

Since Δp_e falls with an increase in swirl, P_2 seldom makes a significant contribution to P.

Estimate for Total Radiated Sound Power

Let $dP_a(\theta)$ denote the energy flux of the sound radiated through an elementary control surface ($dS = 2\pi R^2 \sin\theta\, d\theta$) that is fixed relative to the ambient medium and occupies the sector $(\theta, d\theta)$ of the surface of a large sphere of radius R centered on the jet axis. In the model problem, the ambient medium is in motion, so there are two contributions to dP_a. First, there is the work done on dS by the fluctuating pressure; this is given by $(\overline{p^2}/\rho_a a_a)\,dS$, where $\overline{p^2}$ is the square fluctuating pressure and suffix a denotes the ambient medium. The acoustic energy density is $\overline{p^2}/\rho_a a_a$, so the second contribution is given by $w_c\cos\theta(\overline{p^2}/\rho_a a_a)\,dS$, which represents the flux of acoustic energy through dS. The rotational velocity is tangential to dS and therefore convects no acoustic energy through dS. The two contributions may be added and integrated to give

$$P_a = \frac{2\pi R^2}{(\rho_a a_a)}\int_0^\pi \overline{p^2}(1 - M_a\cos\theta)\sin\theta\, d\theta \tag{47}$$

where $M_a = w_c/a_a$.

In the actual coordinate system, the ambient medium is at rest, so the total sound power radiated into free space is given by

$$P_T = \frac{2\pi R^2}{(\rho_a a_a)}\int_0^\pi \overline{p^2}\sin\theta\, d\theta \tag{48}$$

To estimate P_T/P_a, we make the crude approximation that

$$\overline{p^2} = \text{const}\,(\theta > \theta_p)$$
$$= 0\,(\theta < \theta_p) \tag{49}$$

where θ_p is the peak radiation angle. This approximation is roughly in accordance with experimental observations.[3,4] Using Eq. (49) with Eqs. (47) and (48), we find that

$$\frac{P_T}{P_a} = \int_{\theta_p}^\pi \sin\theta\, d\theta \Big/ \int_{\theta_p}^\pi (1 - M_a\cos\theta)\sin\theta\, d\theta$$
$$= \left[1 + M_a\sin^2\left(\frac{\theta_p}{2}\right)\right]^{-1} \tag{50}$$

P_a can be expected to constitute a fairly high proportion of the energy flux P transferred from the coherent field into the mixing layer. Even that portion of P converted into random internal waves is not completely lost, since some of it is converted to radiated sound after multiple scattering. A certain proportion of energy is lost owing to the dissipation of the random internal wave modes. Therefore, let

$$P_a = KP \tag{51}$$

where the factor of proportionality is expected to be a large fraction. If we assume that K is the same for swirling and nonswirling flows, then recalling that $P = P_1 + P_2$ and using Eqs. (50) and (51) we obtain an expression for the ratio of the total sound powers with and without swirl, viz.,

$$\frac{P_T}{(P_T)_0} = \frac{\left[1 + M_a\sin^2(\theta_p/2)\right]_0}{\left[1 + M_a\sin^2(\theta_p/2)\right]} \cdot \frac{P_1 + P_2}{(P)_0} \tag{52}$$

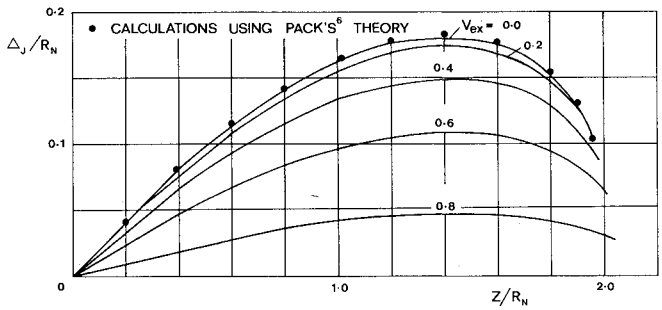

Fig. 6 Jet boundaries for OB swirling flow ($\zeta_c^* = 0.8$, $M_J = 1.4$, $\gamma = 1.4$).

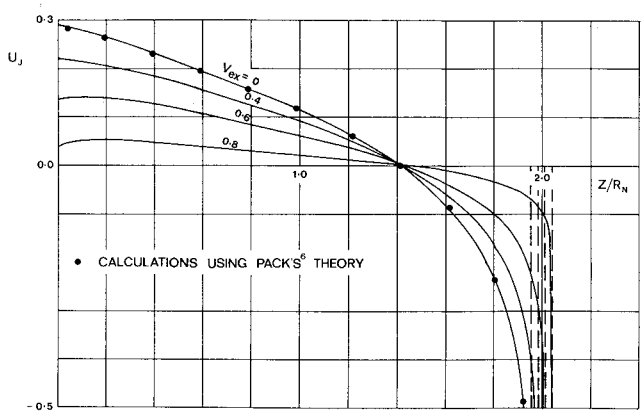

Fig. 7 Normal velocity variation along jet boundary ($\zeta_c^* = 0.8$, $M_J = 1.4$, $\gamma = 1.4$).

Peak Radiation Angle and Frequency

In Ref. 4 equations are derived and solved for $\bar{B}$ and B'. This leads to an expression for $\overline{p^2}$. Within the mixing layer, provided it is thin, the equations for $\bar{B}$ and B' are identical in form for swirling and nonswirling flows. In fact, the only differences between the two cases are the fall in $\bar{w}_j$ (and, hence, reduction of Δp_e) and the change in form of $\bar{u}$ with swirl. The expression for $\overline{p^2}$ is dominated by the singularities in $\bar{u}$, which can be dealt with in a way similar to that above. To determine $\overline{p^2}$ for swirling jets, the changes outlined above are made and Eq. (10.15) of Ref. 4 evaluated. It turns out that θ_p changes very little with swirl (see Table 1) and that the directivity patterns remain fairly similar in shape.

For nonswirling flow, the noise spectra are characterized by a series of peaks, the first of which is given approximately by

$$f_p = w_c/[\lambda|1 - M_a\cos\theta|] \tag{53}$$

This agrees with the semiempirical result of Ref. 3. In view of the above discussion, the spectrum shape would not be expected to change much for swirling flow, so Eq. (53) should still hold. But, since w_c falls with swirl, f_p will change to some extent.

IV. Discussion of Results

In any comparison of flow characteristics with and without swirl it has to be decided what to keep constant. In what follows, the back pressure ratio p_a/p_0 is kept fixed since this

Table 1 Effect of degree and type of swirl on various noise and jet characteristics

Type of flow	V_{ex}	θ_p, deg	$P_2/(P)_0$	A	λ/λ_0	$P_1/(P)_0$	f_pD/W_J
Nonswirling	0.0	77	0.0	0.500	1.000	1.000	0.792
Outer-biased swirl, $\zeta_c^* = 0.8$	0.20	77	−0.0001	0.486	1.002	0.909	0.755
	0.40	76	−0.0003	0.459	1.011	0.603	0.758
	0.60	76	−0.0005	0.414	1.025	0.270	0.664
	0.80	75	−0.0004	0.338	1.042	0.037	0.563
Solid-body rotation, $\zeta_c^* = 0.0$	0.20	77	−0.0001	0.486	1.014	0.918	0.765
	0.40	76	−0.0003	0.444	1.056	0.508	0.721
	0.60	76	−0.0005	0.381	1.122	0.167	0.606
	0.80	75	−0.0004	0.263	1.209	0.033	0.485
Inner-biased swirl, $\zeta_c = 0.8$	0.20	77	−0.0001	0.483	1.029	0.927	0.755
	0.40	76	−0.0003	0.427	1.110	0.514	0.690
	0.60	76	−0.0005	0.275	1.238	0.217	0.549
	0.80	75	−0.0004	0.101	1.414	0.015	0.414

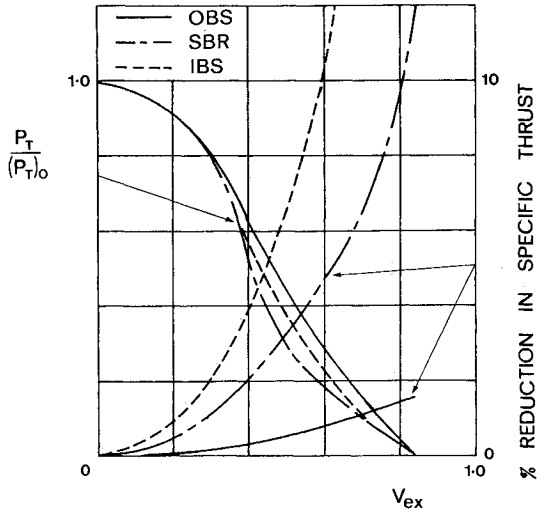

Fig. 8 Effect of swirl on total sound power ($M_J = 1.4$, $\gamma = 1.4$).

corresponds to the situation of most practical interest. If p_a/p_0 is fixed, then the velocity Q_J on the jet boundary will remain constant. Therefore, as the swirl level rises, the axial velocity w_{bJ} falls, as can be seen from Eq. (10). Ultimately, when the swirl level is sufficiently high, w_{bJ} reaches the value w_{ex} and the pressure difference at nozzle exit becomes zero. Under these conditions, the shock cells are presumably completely eliminated. This suggests that swirl has potential as a method for suppressing shock-cell noise.

Numerical results have been obtained for two families of swirl distributions at the nozzle exit. The first of these is defined as

$$V_b = 0: 0 \le \zeta \le \zeta_c^*$$

$$V_b = (\zeta - \zeta_c^*)V_{bJ}/(1 - \zeta_c^*): \zeta_c^* \le \zeta \le 1 \qquad (54)$$

where $\zeta = r_1/R_N$. This represents a flow with a nonswirling core of radius ζ_c^*/R_N surrounded by an annulus of swirling flow. This type of flow could be produced by an annulus of swirler blades and is termed[9] outer-biased swirling (OBS) flow. The second type of swirl is defined as

$$V_b = V_{bJ}\zeta/\zeta_c^2: 0 \le \zeta \le \zeta_c$$

$$V_b = V_{bJ}/\zeta: \zeta_c \le \zeta \le 1 \qquad (55)$$

This represents a swirling flow with a core of radius $\zeta_c R_N$ that is in solid-body rotation; outside the core there is free-vortex flow, termed[9] inner-biased swirling (IBS) flow. The properties of supercritical nozzle flows with these types of swirl are discussed in Refs. 8-10.

Calculations of three different types of swirling flow were carried out by using the linearized theory described in Sec. II. The three types considered were solid-body rotation (SBR), i.e., an OBS flow with $\zeta_c^* = 0$, an OBS flow with $\zeta_c^* = 0.8$, and an IBS flow with $\zeta_c = 0.8$. The Mach number, $M_J = q_J/a_J$, on the jet boundary was set equal to 1.4. The nozzle was assumed to be convergent so that the axial velocity at exit was given by Eqs. (6) and (7). Jet boundaries for the OBS flow are presented in Fig. 6 for various swirl levels and the corresponding normal velocity distributions are presented in Fig. 7. It can be seen from these figures that there is excellent agreement between Pack's theory[6] and the present results when $V_{bJ} = 0$. The relative values of the primary wavelength λ and the coefficient A quantifying the behavior at the logarithmic singularity are given in Table 1 for the three types of swirling flow.

These values of A/A_0 and λ/λ_0 were used in Eqs. (43), (46), and (52) to make estimates of the effect of swirl on the total sound power of shock-associated noise. These results are shown in Fig. 8. Computations were made using Eq. (10.15) of Ref. 4 to determine the change in peak radiation angle θ_p when W_{bJ} is reduced due to swirl with λ kept approximately constant. As can be seen from Table 1, θ_p does not change significantly with swirl. For the purposes of calculating a_a/a_b, it was assumed that within the jet $\gamma = 1.3$ and the stagnation temperature is 1100 K, while in the ambient medium $\gamma = 1.4$ and the temperature is 290 K. This corresponds roughly to the takeoff conditions of an SST like the Concorde. Also plotted in Fig. 8 are estimates of the effect of swirl on specific thrust, calculated using methods described in Refs. 7, 8, and 10. The variation of the peak frequency f_p given by Eq. (53) with swirl is shown in Table 1.

It can be seen from Fig. 8 that in the OBS case for a 1% thrust loss the sound power is reduced to 19% of its nonswirl value. A thrust loss of 1.6% completely eliminates shock-cell noise. These estimates could well be conservative since Smith[13] has published schlieren photographs showing that, at moderate swirl levels, the number of visible shock cells is reduced from six to three. This is probably because of increased turbulent mixing. As well as reducing the shock-cell noise below the present estimates, this reduction in the number of cells should also cause the noise spectra to be more sharply peaked.

V. Conclusions

1) A linearized theory for inviscid supersonic swirling jets has been developed. A simple expression has been derived for

the wavelength of the primary shock cell in a jet with arbitrary initial swirl. Computed jet boundaries and the corresponding distributions of normal velocity are presented.

2) The linearized theory, together with the theory of Howe and Ffowcs Williams for shock-associated noise, is used to make estimates of the effect of swirl on the total radiated sound power of shock-associated noise.

3) It is found that for a certain type of swirl shock-associated noise may be greatly reduced, or even eliminated, for a sufficiently high swirl level. This could be achieved for a very small thrust loss. This suggests that swirl has potential as a method for suppressing shock-cell noise.

References

[1]Powell, A., "On the Mechanism of Choked Jet Noise," *Proceedings of the Physical Society*, Vol. B66, 1953, pp. 1039-1056.

[2]Tam, C.K.W., "On the Noise of a Nearly Ideally Expanded Supersonic Jet," *Journal of Fluid Mechanics*, Vol. 51, Pt. 1, 1972, pp. 69-95.

[3]Harper Bourne, M. and Fisher, M.J., "The Noise from Shock Waves in Supersonic Jets," AGARD CP-131, 1973, Paper 11.

[4]Hower, M.S. and Ffowcs Williams, J.E., "On the Noise Generated by an Imperfectly Expanded Supersonic Jet," *Philosophical Transactions of the Royal Society*, Vol. A289, 1978, pp. 271-314.

[5]Prandtl, L., "Uber die stationären Wellen in einem Gasstrahl," *Physikalische Zeitschrift*, Vol. 5, 1904, pp. 599-601.

[6]Pack, D.C., "A Note on Prandtl's Formula for the Wave-Length of a Supersonic Gas Jet," *Quarterly Journal of Mechanics and Applied Mathematics*, Vol. 3, 1950, pp. 173-181.

[7]Carpenter, P.W. and Johannesen, N.H., "An Extension of One-Dimensional Theory to Inviscid Swirling Flow through Choked Nozzles," *Aeronautical Quarterly*, Vol. 26, May 1975, pp. 71-87.

[8]Carpenter, P.W., "The Effects of Swirl on the Performance of Supercritical Convergent-Divergent Nozzles," *Aeronautical Quarterly*, Vol. 32, May 1981, pp. 126-152.

[9]Carpenter, P.W., "A General One-Dimensional Theory of Compressible Inviscid Swirling Flows in Nozzles," *Aeronautical Quarterly*, Vol. 27, Aug. 1976, pp. 201-216.

[10]Carpenter, P.W., "Supercritical Swirling Flows in Convergent Nozzles," *AIAA Journal*, Vol. 19, May 1981, pp. 657-660.

[11]Grabitz, G., "Analytische Lösung für den stationären rotationssymmetrischen Überschall-Freistrahl in linearer Näherung," *Zeitschrift für Angewandte Mathematik und Mechanik*, Vol. 55, April 1975, pp. T127-T130.

[12]Carpenter, P.W., "A Small Perturbation Theory for Supersonic Jets," AIAA Paper 78-1151, July 1978.

[13]Smith, R., "An Investigation of Supersonic Swirling Jets," *Aeronautical Quarterly*, Vol. 24, Aug. 1973, pp. 167-178.